Is CoMP Beneficial In User-Centered Wireless Networks?

Shahrukh Khan Kasi*, Umair Sajid Hashmi†, Muhammad Nabeel*, Sabit Ekin‡, Ali Imran*

*AI4Networks Research Center, School of Electrical & Computer Engineering, University of Oklahoma, USA.
†School of Electrical Engineering & Computer Science, National University of Sciences & Technology, Pakistan
‡School of Electrical & Computer Engineering, Oklahoma State University, USA

*{shahrukhkhankasi, muhmd.nabeel, ali.imran}@ou.edu, †umair.hashmi@seecs.edu.pk, ‡sabit.ekin@okstate.edu

Abstract—This paper investigates the benefit of coordinated multipoint transmission (CoMP) in a User-Centered Cloud-based Radio Access Network (UC-CRAN). In UC-CRAN, virtual cells (also called service zones) are created around a user effectively changing the center of network operation from "always ON" base stations to user demands. The user-centered architecture potentially removes cell-edge users due to the spatial repulsion between service zones, thereby limiting the potential of CoMP which is effective in networks with cell-edge interference. To this end, we derive an analytical framework to model the area spectral efficiency (ASE) and energy efficiency (EE) in UC-CRAN with CoMP. Further, the investigation encompasses analyzing the impact of CoMP in UC-CRAN on ASE and EE with the change in service zones size and data base station (DBS) deployment density. The proposed analytical method is validated using extensive Monte Carlo simulations providing useful insights for the design of next-generation cellular networks.

Index Terms—CoMP, user-centered, CRAN, ASE, EE.

I. INTRODUCTION

A. Motivation

Small cells deployed densely in heterogeneous networks (HetNets) provide unprecedented network coverage and capacity, but at the expense of increased inter-cell interference and increased costs to network operators [1]. UC-CRAN, which creates service zones around scheduled users and separates the core baseband processing unit from the radio access unit, addresses the challenges posed by HetNets [2].

Architecturally, UC-CRAN is best suited to support CoMP solutions which have the ability to enhance key performance indicators (KPIs) in a wireless network [3]. While the main benefits of incorporating CoMP into wireless networks are to address cell-edge interference, the UC-CRAN architecture is capable of eliminating cell-edge users by re-orienting the network design from base station to user [4]. Considering these opposing characteristics, we hypothesize that using CoMP in the UC-CRAN architecture will not improve key performance metrics, such as coverage probability, ASE, EE.

To this end, we integrate the CoMP solution into the user-centered architecture we proposed in our previous publications [5], [6] and provide an analysis of ASE, and EE of UC-CRANs with CoMP. As part of our analysis, we analyze how the network elasticity offered by the UC-CRAN architecture impacts ASE and EE. This paper discusses the impact of network-level control parameters on the system-level KPIs,
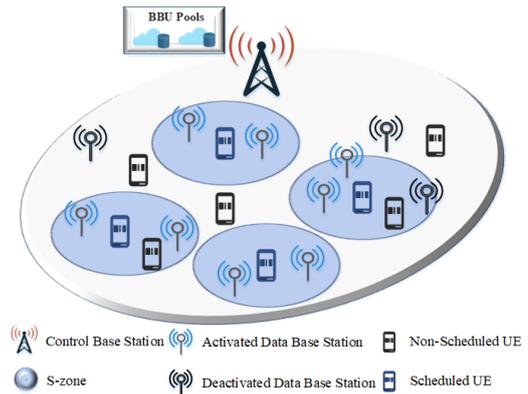
Fig. 1: CoMP-enabled UC-CRAN architecture.

providing insights into the inclusion of CoMP in UC-CRAN and the design and planning of future networks.

B. Related Work

The CoMP paradigm has been incorporated and studied in various HetNets for the last two decades [7]. Despite this, few CoMP solutions have been offered for UC-CRAN architecture. The authors of [8] derived an analytical formula for coverage probability, together with two approximations, for cooperative usage of base stations in the downlink HetNet. While the authors have emphasized the coverage probability analytical model, they gave no insight into how CoMP impacts other KPIs in a user-centered network.

Authors of [9] developed a max-min rate method to minimize UC-CRAN's power consumption by optimizing beam-forming weights and access point-user equipment association together. Authors in [10] have used the similar approach to jointly solve the user association and remote radio head activation problems in dense CRANs by increasing the number of users serviced while ensuring a minimal data rate requirement and then maximising system throughput.

In contrast to existing studies, the proposed analytical framework examines ASE and EE in the context of a CoMP-enabled UC-CRAN architecture and gives a close bound to numerical results. Based on the analytical framework, the optimal size of the S-zone and DBS density is determined in terms of ASE and EE.

C. Contributions

In summary, the contributions of this work are as follows:

- Using stochastic geometry tools, we analyze the activated DBS density and average aggregated interference in UC-CRAN with integrated CoMP based on UC-CRAN architecture proposed in [5], [6].
- A closed-form expression is derived quantitatively for a scheduled UE in a CpMP-enabled UC-CRAN, expressing the coverage probability, ASE, and EE.
- Furthermore, we examine the impacts of network elasticity provided by UC-CRAN, i.e., the S-zone size and DBS density, on ASE and EE of CoMP-enabled UC-CRAN.

D. Paper Organization and Notation

In this paper, the boldface small case letter $\mathbf{x}$ represents a vector, and $||\mathbf{x}||$ represents the $L2$ norm of vector $\mathbf{x}$ in Euclidean space. $/$ represents the set subtraction, whereas $\in$ represents membership in the set. For random variables Z, $\mathbb{E}_Z(.)$ and $f_Z(.)$ are used to denote the average value and the probability density function, respectively. A uniform distribution between a and b is indicated by the symbol $Z \sim U(a,b)$. An exponential distribution with an average value μ is indicated by the symbol $Z \sim e^\mu$. A characteristic function is represented by the $\mathbb{1}(x > y)$ symbol, while $b(x,r)$ is a circle centered at a point x with a radius of size r.

The remainder of the paper is organized as follows. Section II discusses the network model. Section III quantifies KPIs such as ASE and EE using an analytical framework. Section IV evaluates the analytical framework. Finally, Section V summarizes the outcomes of the paper.

II. NETWORK MODEL

As part of the UC-CRAN model, arbitrary UEs are scheduled based on their service requirements, and S-zones are created around all UEs at the start of each transmission time interval (TTI). One or more DBS can be activated within an S-zone to provide coverage to a specific scheduled UE. Scheduled UEs may be served by different DBSs across different TTIs subject to the variation in user movement, spatial distribution of DBSs, and environmental conditions. It is necessary to use a mechanism for cooperation if more than one DBS is activated simultaneously to service a UE.

Based on implementation complexity and bandwidth requirements, the 3GPP identified three major downlink coordination schemes for 5G [11]. 5G CoMP schemes can be classified as: (i) joint transmission (JT), (ii) coordinated beamforming (CB), and (iii) dynamic point selection (DPS). With JT, channel state information (CSI) and user data are exchanged between coordinated transmission points. A CB transmission requires only the CSI to be shared, while DPS requires the data to be transmitted by only one transmission point at a specific TTI. Though JT offers the maximum gain in performance, it also has the highest bandwidth requirement of all coordination schemes [3].

Here we mainly concentrate on implementing JT for cooperative DBS transmission. As a rule of thumb, at a specific TTI,

the maximum number of cooperative transmission points in an S-zone cannot exceed $M \in Z^+$, where Z^+ is a set of positive integers. A fixed number of cooperating DBSs is not assumed due to the random spatial distribution of DBSs, i.e., there will be S-zones that have less than M DBSs present in its region. Further, each scheduled UE is serviced by at most M DBSs, providing the most significant channel gain within the S-zone region. Fig. 1 illustrates a UC-CRAN with a maximum of two cooperative DBSs. When there are less than or equal to two DBSs in an S-zone, all DBSs cooperate to offer coverage to a scheduled UE. If there are more than two DBSs in an S-zone, only those providing the most significant channel cooperate to offer coverage to a scheduled UE.

A. Channel Model

The present work considers a cloud-based radio access network with ultra-dense DBS deployment, which is a scenario possible for future networks. UEs and DBSs are spatially modeled as independent stationary Poisson point processes Π_{UE} and Π_{DBS} with densities λ_{UE} and λ_{DBS}, respectively. The average number of DBSs in an S-zone can be approximated by $\lambda_{DBS}\pi R_{szone}^2$, which is the Lebesgue radius of a disc with radius R_{szone} [12].

The communication channel between an arbitrary UE $x \in \Pi_{UE}$ and DBS $y \in \Pi_{DBS}$ can be described by $h_{xy}\ell(||x-y||)$ with $h_{xy} \sim e^1$ being a unit mean exponential random variable representing the effects of Rayleigh fading, and $\ell(||x-y||)$ being the large-scale path loss model. In the large-scale path loss model, the path loss exponent and distance between the UE and DBS $||x-y||$ are taken into account along with a frequency-dependent constant K. The DBSs are assumed to transmit at equal power, and UEs and DBSs have one antenna only.

B. User-centered Clustering in UC-CRAN

The user-centered cluster mechanism given in [5], [6] is utilized in this work. The macro-cell or BBU schedules the UEs at each TTI according to their scheduling priorities. Scheduling is performed on UEs iff their scheduling priority is the highest in their cluster radius, which is defined as R_{szone}. Furthermore, any two S-zones should be at least $2R_{szone}$ apart. It should be noted that this circle (S-zone) corresponds to the size of the cooperative cluster. A dynamic change in size of an S-zone allows flexible activation of DBSs within an S-zone to serve a scheduled UE based on the cooperation scheme used. Macro-cells or BBUs are responsible for both activating DBSs in a cooperative cluster and delegating the size of clusters to UEs. UC-CRAN utilizes on-demand activation of DBSs to self-organize its coverage based on the spatiotemporal variation in user demographics.

C. Signal Model

In our model, we are considering a scheduled UE $x \in \Pi'_{UE}$, where Π'_{UE} represents the distribution of scheduled UEs. Due to the repulsion between adjacent scheduled UEs, Π'_{UE} can

be modeled as a type II Matern hardcore process. We can approximate the density of scheduled UEs as follows [12]:

$$\lambda'_{UE} = \frac{1 - e^{-\lambda_{UE}4\pi R_{szone}^2}}{4\pi R_{szone}^2}. \quad (1)$$

Let $\Pi'^C_{DBS} = \Pi'_{DBS} \cap b(x, R_{szone})$ be a set of activated DBSs serving scheduling UE x based on its scheduling criteria [5]. The spatial distribution of activated DBSs is given by Π'_{DBS} and the set of interfering DBSs can be given as $\Pi'^I_{DBS} = \Pi'_{DBS} \backslash \Pi'^C_{DBS}$. It is sufficient to analyze a typical UE due to the stationarity of the PPP of scheduled UE. A single point added to the origin does not alter the stationarity of a PPP, which is why a probe UE is placed at the origin [12].

III. KPI CHARACTERIZATION IN UC-CRAN

Within an S-zone of area $b(o, R_{szone})$, a typical UE is served by at most M activated DBSs with UE centered at the origin o. According to this definition, a cooperative cluster can be expressed as:

$$C = arg_{r_1, r_2, \dots, r_n \subset \Pi'_{DBS}} \sum_{i=1}^n h_i r_i^{-\alpha}, \quad (2)$$

where $n \leq M$, r_i is the measure of Euclidean distance between scheduled UE and activated DBS, h_i is the small-scale fading component and Π'_{DBS} is an homogenous PPP representing DBS distribution with the density of λ'_{DBS}. The CoMP JT mode allows all transmission points to broadcast a message at the same time-frequency resource to a scheduled user. As a result, in an interference-limited environment the signal-to-interference ratio (SIR) can be expressed as follows:

$$SIR = \Gamma_{UE} = \frac{\sum_{i \in \Pi'^C_{DBS}} h_i r_i^{-\alpha}}{\sum_{j \in \Pi'^I_{DBS}} h_j r_j^{-\alpha}}. \quad (3)$$

Due to the noise power being much lower than the aggregate interference experienced by each scheduled UE, it is valid to assume that an interference-limited environment exists [8].

A. Expected Interference & Density of Activated DBSs

A typical UE's expected interference, based on the Slivnyak's theorem and Palm measure [12], is expressed as:

$$\mathbb{E}_{\mathbf{I}}[I] = \frac{2\pi\lambda'_{DBS}}{(\alpha-2)(R_{szone}^{\alpha-2})}, \quad (4)$$

where λ'_{DBS} is the density of activated DBSs. This density can be approximated by $p_{ACT}\lambda_{DBS}$ with p_{ACT} representing the activation probability of DBSs in an S-zone. p_{ACT} can be calculated as follows:

$$p_{ACT} = \left(1 - e^{-\lambda'_{UE}\pi R_{szone}^2}\right) \cdot \left(\frac{\Gamma(M+1, X)}{\gamma(M+1)} + e^{-X}\right.$$
$$\left[\frac{M(X)^{M+1}{}_2F_2(1, M+1; M+2, M+2; X)}{(M+1)\gamma(M+2)} - 1\right]\right), \quad (5)$$

where $_pF_q(a_1, \dots, a_p; b_1, \dots, b_q; z)$, $\gamma(x)$, $\Gamma(x, y)$, and $X = \lambda_{DBS}\pi R_{szone}^2$, correspond to the generalized hypergeometric function, complete gamma function, upper incomplete gamma function, and the mean number of DBSs in an S-zone, respectively.

B. Coverage Probability

In general, the probability of a UE receiving SIR greater than a certain threshold (γ_{th}) defines its coverage probability. It can be expressed mathematically as follows:

$$P_{cov}(\gamma_{th}, R_{szone}) = 1 - \mathbb{E}_{\mathbf{I}}\left[P_r\left(S < \gamma_{th}I\right)\right], \quad (6)$$

where the desired signal power and the aggregated interference strength are represented by $S = \sum_{i \in \Pi'^C_{DBS}} h_i r_i^{-\alpha}$ and $I = \sum_{j \in \Pi'^I_{DBS}} h_j r_j^{-\alpha}$, respectively.

Theorem 1. In a CoMP-enabled UC-CRAN, the lower bound on the coverage probability for a typical user is given as follows:

$$P_{cov}(\gamma_{th}, R_{szone}) \geq 1-$$
$$\exp\left(-\frac{\lambda_{DBS}\pi^{1-\delta}\delta\gamma\left(\delta, \frac{\gamma_{th}2\pi\lambda'_{DBS}R_{szone}^2}{\alpha-2}\right)}{(\gamma_{th}2\lambda'_{DBS})^\delta(R_{szone})^{-\delta(\alpha-2)}(\alpha-2)^{-\delta}}\right), \quad (7)$$

where $\delta = \frac{2}{\alpha}$ and $\gamma(a, b) = \int_a^b t^{a-1}e^{-t}dt$ is the lower incomplete Gamma function.

Proof: A UE is serviced successfully if the SIR received at a typical UE exceeds the minimum SIR threshold. The relationship between the void probability of modified active DBS ($P_r(\Pi'_{DBS} = \emptyset)$) and coverage probability $Pr(S > \gamma_{th}I)$ can be determined with the concepts of thinned marked PPP [12].

$$P_r\left(S > \gamma_{th}I\right) = 1 - P_r\left(S < \gamma_{th}I\right)$$
$$= 1 - P_r(\Pi'_{DBS} = \emptyset) = 1 - e^{-\Lambda(B)}, \quad (8)$$

where the average measure $\Lambda(B)$ can be evaluated according to the concepts described in [12]:

$$\Lambda(B) = \int_0^{R_{szone}} \int_0^\infty 2\pi\lambda_{DBS}r\mathbb{1}(hr^{-\alpha} \geq \gamma_{th}I)f_H(h)dhdr$$
$$\stackrel{(a)}{=} 2\pi\lambda_{DBS}\int_0^{R_{szone}} rP_r(h \geq \gamma_{th}Ir^\alpha)dr$$
$$\stackrel{(b)}{=} \frac{\pi\lambda_{DBS}\delta\gamma(\delta, \gamma_{th}IR_{szone}^\alpha)}{\gamma_{th}^\delta I^\delta}, \quad (9)$$

where (a) expresses the cumulative distribution function of an exponential random variable, and (b) expresses the integration by taking variable $t = \gamma_{th}Ir^\alpha$.

By substituting Eq. (8) into Eq. (9) and applying Jensen's inequality, the lower bound for coverage probability will be as follows:

$$P_{cov}(\gamma_{th}, R_{szone}) \geq 1 - e^{-\frac{\lambda_{DBS}\pi\delta\gamma(\delta, \gamma_{th}\mathbb{E}_{\mathbf{I}}[I]R_{szone}^\alpha)}{\gamma_{th}^\delta\mathbb{E}_{\mathbf{I}}[I]^\delta}}. \quad (10)$$

A proof of the above expression is concluded by using the value of $\mathbb{E}_{\mathbf{I}}[I]$ in Eq. (4).

Symbol	Parameter Name	Parameter Value
-	Simulation Area	$100\,m \times 100\,m$
λ_{UE}	UE's density	$10^{-1}/m^2$
λ_{DBS}	DBS's density	$10^{-2} - 10^{-1}/m^2$
α	Path-loss exponents	3
R_{szone}	Radius of S-zone	$1\,m - 10\,m$
M	Max Cooperative DBSs	$1 - 5$

TABLE I: Simulation Parameters.
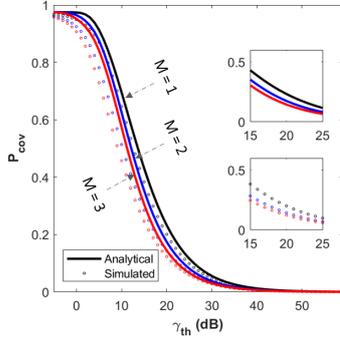
Fig. 2: Coverage probability for different γ_{th} and M.

C. ASE

The lower bound on ASE considers the transmission with the rate of $\log_2(1 + \gamma_{th})$ for all users [13].

$$ASE = \lambda'_{UE} \log_2(1 + \gamma_{th}) P_{cov}(\gamma_{th}, R_{szone}). \quad (11)$$

D. EE

EE can be expressed as [5]:

$$EE = \frac{\log_2(1 + \Gamma_{cran})}{P_{cran}}, \quad (12)$$

where P_{cran} represents the average network power consumption and Γ_{cran} represents the effective SIR [5]. When modeling power consumption, we mainly consider the overhead associated with: (i) enabling cooperation between transmission points, and (ii) discovering the DBSs offering the most significant channel gains. The inspiration for modeling power consumption comes from the works in [14] in which the authors incorporate power associated with power amplifies, baseband processing, temperature control, and antenna interfacing. The network power consumption is, therefore, as follows:

$$P_{cran} = P_O + P_{sp} + \Delta_u P_u + P_{ou}, \quad (13)$$

where the power consumption of DBS in listening mode is P_O, the UE transmission power is P_u, the power consumption associated with radio frequency components of the UE is Δ_u, the power dissipated at the UE circuits is P_{ou}, and the signal processing overhead is P_{sp}.

IV. SYSTEM EVALUATION

MATLAB simulations are used to assess the performance of the CoMP-enabled UC-CRAN with the simulation parameters specified in Table I. Monte Carlo simulations are executed with 10^4 realizations in each experiment.

A. Coverage Probability Validation

For both CoMP and no-CoMP scenarios, Fig. 2 shows the analytical and experimental results for the coverage probability for different values of γ_{th}. The analytical coverage probability serves as a lower bound to the experimental coverage probability (as discussed in Section III) and the coverage probability decreases as γ_{th} is increased.

Fig. 2 showcases interesting observation: the difference in coverage probabilities between UC-CRAN architectures with CoMP-enabled and no-CoMP. Recall that the UC-CRAN architecture eliminates cell-edge users meaning that the significant benefit of CoMP, which is to mitigate the cell-edge interference is no longer applicable. If there are no cell-edge UEs, the inclusion of CoMP can only improve the received signal power at a scheduled UE. Nonetheless, if the DBSs are activated based on their channel gains, the DBS with the most significant channel gain will always be the most influential contributor to the received signal power at a scheduled UE. Consequently, enabling the CoMP increases the received signal power by a small fraction due to the difference in channel gains arising from the random spatial distribution of DBSs and path-loss scaling. In contrast, the average interference will increase linearly as more DBSs are activated in CoMP, resulting in decreased coverage probability at a scheduled UE.

B. Optimizing S-zone Radius and DBS Density

The ASE is plotted for different values of the S-zone radius and M in Fig. 3 (a). Based on our hypothesis, an optimal S-zone radius maximizes ASE, and the S-zone radius maximizing ASE should be smaller than the S-zone size maximizing EE. Increasing the S-zone radius decreases the number of scheduled UEs, affecting the network ASE. Furthermore, a decrease in the S-zone radius may lead to densely populated scheduled users at the risk of spatially closer S-zones, leading to an increase in cumulative interference levels. As a result, the optimal radius for the S-zone should be a small value but not too small to maximize ASE. In Fig. 3 (a), the optimal S-zone radius to maximize ASE is 1.5 m, slightly larger than the minimum considered S-zone radius of 1 m. This confirms the hypothesis discussed above. A consistent trend in terms of ASE can also be observed across different M.

Besides the S-zone radius, the density of DBSs is also a significant design parameter from the viewpoint of a mobile network operator. Fig. 3 (b) plots ASE for a range of DBS densities and maximum cooperators, where the monotonic increase in ASE can be observed with the increase in DBS density. This is in part because with dense DBS deployment, (i) the possibility of coverage holes due to the absence of DBS in an S-zone decrease, and (ii) there are more options to activate the DBS(s) with better channel gains.

Lastly, network EE is plotted in Fig. 4 for different S-zone radius and M values. Similar to ASE, there exists an S-zone radius for which the EE will be maximized. Although, the S-zone radius that would maximize EE will not be the same as that that would maximize ASE. A larger S-zone radius would maximize EE intuitively because a larger S-zone radius leads
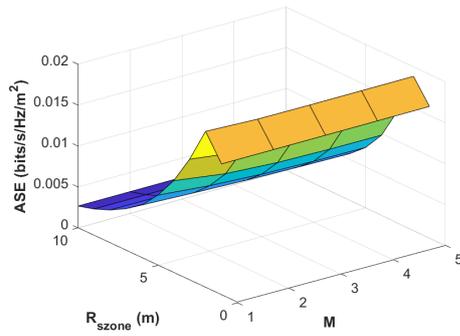
(a) $\lambda_{DBS} = 0.03$.
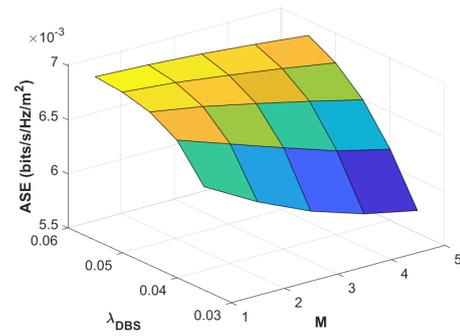
(b) $R_{szone} = 6m$.

Fig. 3: ASE of the CoMP-enabled UC-CRAN.
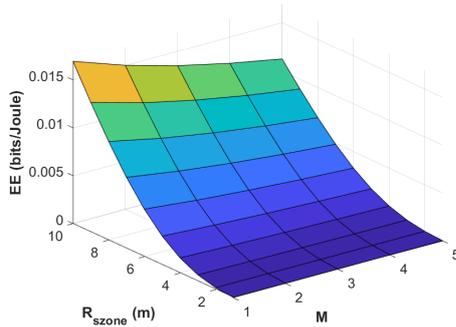
Fig. 4: EE of the CoMP-enabled UC-CRAN.

to a reduced density of activated DBSs, resulting in lesser power consumption. Combined with the observations in Fig. 3, we can conclude that the S-zone radius, DBS density, and the number of cooperative DBSs strongly affect ASE and EE. A self-organizing framework should be used to jointly optimize all of these inter-linked parameters to maximize ASE and EE.

V. CONCLUSION

This paper analyzes the impact of enabling cooperation between transmission points in a UC-CRAN architecture with an analytical and experimental study. Using extensive Monte Carlo simulations, we showed that using CoMP in a UC-CRAN architecture reduces not only network EE but also the probability of coverage at a scheduled UE, thereby reducing the network ASE. Our analysis validates the claim implicitly discussed in the literature but not fully explored that the real gains introduced by CoMP can be observed in networks with cell-edge users. This work presents a baseline for the design and planning of future networks. The complete version of this work has been published as a transaction paper [15].

REFERENCES

[1] R. Oughton, "Assessing the capacity, coverage and cost of 5G infrastructure strategies," *Telematics and Informatics*, vol. 37, pp. 50–69, 2019.

[2] A. Checko, H. L. Christiansen, Y. Yan, L. Scolari, G. Kardaras, M. S. Berger, and L. Dittmann, "Cloud ran for mobile networks—a technology overview," *IEEE Communications surveys & tutorials*, vol. 17, no. 1, pp. 405–426, 2014.

[3] S. Bassoy and A. Imran, "Coordinated Multi-Point Clustering Schemes: A Survey," *IEEE Communications Surveys and Tutorials*, vol. 19, no. 2, pp. 743–764, 2017.

[4] S. Chen, T. Zhao, H. H. Chen, Z. Lu, and W. Meng, "Performance analysis of downlink coordinated multipoint joint transmission in ultra-dense networks," *IEEE Network*, vol. 31, no. 5, pp. 106–114, 2017.

[5] U. S. Hashmi, S. A. R. Zaidi, A. Imran, and A. Abu-Dayya, "Enhancing Downlink QoS and Energy Efficiency Through a User-Centric Stienen Cell Architecture for mmWave Networks," *IEEE Transactions on Green Communications and Networking*, vol. 4, no. 2, pp. 387–403, 2020.

[6] U. S. Hashmi, S. A. R. Zaidi, and A. Imran, "User-centric cloud ran: An analytical framework for optimizing area spectral and energy efficiency," *IEEE Access*, vol. 6, pp. 19 859–19 875, 2018.

[7] A. H. Sakr and E. Hossain, "Location-aware cross-tier coordinated multipoint transmission in two-tier cellular networks," *IEEE Transactions on Wireless Communications*, vol. 13, no. 11, pp. 6311–6325, 2014.

[8] N. Guo, M.-L. Jin, and N. Deng, "Coverage analysis for heterogeneous network with user-centric cooperation," *IEEE Systems Journal*, vol. 13, no. 3, pp. 2724–2727, 2018.

[9] J. Shi, H. Xu, Z. Yang, and M. Chen, "Energy efficient beamforming for user-centric virtual cell networks," *IEEE Transactions on Green Communications and Networking*, vol. 3, no. 3, pp. 575–590, 2019.

[10] Z. Wu, Z. Fei, Z. Zheng, B. Li, and Z. Han, "Remote radio head activation and user association in dense c-rans," *IEEE Transactions on Vehicular Technology*, vol. 69, no. 10, pp. 12 216–12 228, 2020.

[11] T. R. 36.819, "Coordinated Multi-Point Operation for LTE Physical Layer Aspects," 2013.

[12] S. N. Chiu, D. Stoyan, W. S. Kendall, and J. Mecke, *Stochastic geometry and its applications*. John Wiley & Sons, 2013.

[13] A. AlAmmouri, J. G. Andrews, and F. Baccelli, "SINR and throughput of dense cellular networks with stretched exponential path loss," *IEEE Transactions on Wireless Communications*, vol. 17, no. 2, pp. 1147–1160, 2017.

[14] G. Auer, V. Giannini, C. Desset, I. Godor, P. Skillermark, M. Olsson, M. A. Imran, D. Sabella, M. J. Gonzalez, O. Blume *et al.*, "How much energy is needed to run a wireless network?" *IEEE Wireless Communications*, vol. 18, no. 5, pp. 40–49, 2011.

[15] S. K. Kasi, U. S. Hashmi, M. Nabeel, S. Ekin, and A. Imran, "Analysis of area spectral & energy efficiency in a comp-enabled user-centric cloud ran," *IEEE Transactions on Green Communications and Networking*, 2021.